Binary Activity Coefficients from Microdroplet Evaporation

Asit K. Ray and Sankar Venkatraman
Dept. of Chemical Engineering, University of Kentucky, Lexington, KY 40506

A method-based on evaporation of a constant-composition droplet containing two components that differ markedly in volatility accurately estimates activity coefficients of both components. This new technique is developed to simultaneously determine the evaporation rate and composition of a droplet from intensity peaks observed in the light scattered by the droplet. It has no upper or lower limits on the relative volatility of the system and is particularly suitable for systems containing one relatively nonvolatile component. The data on the glycerol-ethanol system, obtained from evaporation of glycerol droplets in ethanol vapor and correlated with Margules and Wilson equations, are thermodynamically consistent. The results of this study agree with ethanol activity coefficients calculated from the total pressure vs. solution composition data previously reported.

Introduction

Multicomponent phase equilibrium properties are important in designing many industrial processes and understanding numerous natural phenomena. It is not feasible to measure vapor-liquid equilibrium data for systems containing many components. Usually, the properties of such systems are predicted from excess Gibbs free energy models containing two or more parameters. The model parameters are normally evaluated from experimental data on binary systems. The accuracy of this approach depends on the precision of binary vapor-liquid equilibrium data.

The activity coefficients of a binary system can be measured using several techniques that include: (i) measurement of isothermal equilibrium total pressure vs. composition data; (ii) dynamic and differential ebulliometry (Swietoslawski, 1945; Palczweka-Tulinska et al., 1990; Eckert et al., 1981; Lobien and Prausnitz, 1982; Trampe and Eckert, 1990; (iii) dynamic gas chromatography (Pescar and Martin, 1966; Malik, 1976; Donohue et al., 1985); and (iv) headspace chromatography (Hackenberg and Schmidt, 1976; Cheong and Carr, 1990; Li et al., 1990). These techniques can be used to obtain activity coefficients of both components of a wide variety of binary systems. However, these techniques only provide the activity coefficient of the more volatile component of a system with very low relative volatility, and are not suitable when both components are relatively nonvolatile.

Recently, Trampe and Eckert (1993) developed a technique based on the dew point measurement of a vapor phase of known constitution. The technique is best suited for measuring the limiting activity coefficient of the less volatile component of a system with low relative volatility. Due to the limitations in the construction of a vapor phase of known composition and in the temperature measurement, the method is suitable for a system with relative volatility in the range of 0.3 to 10^{-5}.

Over the last few years, a new method based on the electrodynamic balance has been applied to measure activity coefficients of water in salt solutions (Richardson and Kurtz, 1984; Kurtz and Richardson, 1984; Richardson and Spann, 1984; Tang et al., 1986; Cohen et al., 1987a,b). In this method, the weight change of a single salt particle suspended in an electrodynamic balance is measured as the total pressure due to water vapor is increased.

Recently, Allen et al. (1990) have shown that measurements on a binary solution microdroplet evaporating in a vapor-free atmosphere inside an electrodynamic balance can be used to determine activity coefficients of two relatively nonvolatile components. They have used weight change and scattered intensity data to determine the droplet size and composition, and interpreted the results using quasi-steady-state

Correspondence concerning this article should be addressed to A. K. Ray.

mass flux relations. The technique is only suitable for systems with nonvolatile components. When one or both components of a droplet are volatile, the evaporation process is nonisothermal, and the interpretation of data (determination of the droplet size, composition and temperature as functions of time from simultaneous differential equations) becomes tedious.

For systems with components that differ markedly in volatility, the conventional measurement methods do not provide any information on the activity coefficient of the less volatile component. For example, in the analysis of isothermal total pressure vs. composition data, one neglects the contribution of the less volatile component to obtain the activity coefficient of the more volatile component. For the less volatile component, as the results from prior studies show, only fragmented data such as limiting activity coefficients may be directly determined from, for example, dew point measurements (Trampe and Eckert, 1993).

The purpose of this study is to demonstrate that the activity coefficients of both components, differing markedly in volatility, can be determined from measurements on a binary solution droplet evaporating in a vapor phase that is free of the less volatile component but contains known concentration of the more volatile component. During the quasi-steady evaporation, such a droplet evaporates as a constant-composition solution droplet. When the vapor pressure of the less volatile component is sufficiently low, the droplet remains at a dynamic equilibrium with the more volatile component in the gas phase, and the evaporation rate is dictated by the activity of the less volatile component. Thus, from the quasi-steady composition and evaporation rate, one can simultaneously determine the activity coefficients of both components. In the present study, the composition and evaporation rate of a droplet are determined using a light scattering technique. In this article we present results on single glycerol droplets evaporating in partially saturated ethanol vapor inside an electrodynamic balance, and show that the measurements are thermodynamically consistent. The theory and experiments presented here demonstrate that measurements on droplet evaporation in controlled environments provide accurate vapor-liquid equilibrium data for a wide range of binary systems.

Theory

Mathematical models for evaporation and growth of multicomponent droplets are usually formulated under a quasi-steady assumption (Newbold and Amundson, 1973; Renninger et al., 1981; Smolik and Vitovec, 1984). Huckaby and Ray (1989) and Vijayaragahavan (1990) have rigorously examined the growth and evaporation of binary droplets under unsteady conditions by considering gas and droplet phase heat and mass transport as well as nonideal solution behavior. When a droplet is suddenly exposed to a gas phase, their results show that after an initial unsteady period the system attains a quasi-steady state, marked by uniformity of composition inside the droplet. In the quasi-steady state, the droplet evaporates or grows as a constant composition mixture (the composition of the droplet does not change with time). Thus, for a binary droplet of components A and B, evaporating in a stagnant environment that contains a nontransferring species C (such as, air), the following relation holds during the quasi-steady period:

$$\frac{N_{As}}{N_{Bs}} = \frac{x_A}{x_B} \tag{1}$$

To develop a solution for the quasi-steady period, we make the following assumptions:

- The total molar density, thermal conductivity of the gas mixture and effective diffusivities are independent of temperature and concentration variations.
- The droplet size and system pressure are such that the continuum theory applies.
- The droplet-gas interface remains at equilibrium at all times, and the equilibrium can be described by the vapor-liquid equilibrium relations for bulk systems (that is, $p_i = \gamma_i x_i P_i^0$). This assumption implies that there is no interfacial resistance, and that the droplet is sufficiently large at all times to justify the neglect of the curvature effect (that is, Kelvin effect)

Under the above assumption, the steady-state heat and mass-transfer equations can be solved to obtain the temperature and concentration distributions in the gas phase surrounding the droplet. Using the gas-phase temperature and concentration distributions along with the interfacial conditions and Eq. 1, one may obtain the following simultaneous equations for the droplet temperature and composition:

$$T_s = T_\infty + \frac{\Delta H_{vM}}{C_{pM}} \left\{ 1 - \left(\frac{1 - p_{A_\infty}/x_A P_t}{1 - \gamma_A P_A^0(T_s)/P_t} \right)^{Le} \right\} \tag{2}$$

and

$$\frac{1 - P_{B_\infty}/x_B P_t}{1 - \gamma_B P_B^0(T_s)/P_t} = \left(\frac{1 - p_{A_\infty}/x_A P_t}{1 - \gamma_A P_A^0(T_s)/P_t} \right)^{D_{AM}/D_{BM}} . \tag{3}$$

A material balance at the droplet-gas interface provides the following relation for the droplet radius as a function time:

$$a^2 = a_0^2 - \frac{2 D_{AM} c_t M_A x_A}{\rho w_A} \ln \left(\frac{P_t - p_{A_\infty}/x_A}{P_t - \gamma_A P_A^0(T_s)} \right) (t - t_0). \tag{4}$$

Physical acceptable solutions of Eqs. 2 and 3 exist for the evaporation of a droplet under various scenarios. For experimental purposes, however, some of the solutions are not quite as meaningful as others. For example, when a droplet containing components that differ markedly in volatility evaporates in a vapor-free atmosphere, the mole fraction of the volatile component in the constant-composition droplet in the quasi steady may be negligibly small. For all practical purposes, the droplet evaporates as a pure droplet of the less volatile component. However, when a binary droplet evaporates in a gas phase that is devoid of the less volatile component but contains the more volatile component, the composition of the droplet is dictated by the bulk gas partial pressure of the more volatile component. Thus, the droplet composition can be varied in a controlled manner by systematically

altering the partial pressure of the more volatile component, and the activity coefficients of both components as functions of composition can be determined.

The results of the above analysis simplify considerably if the less volatile component is relatively nonvolatile. For discussion purposes we shall denote the less volatile component as A. For $P_A^0/P_t \leq 10^{-5}$, the droplet temperature can be assumed to be equal to the bulk gas temperature, and in an A-free atmosphere Eqs. 3 and 4 simplify to

$$\beta\gamma_A x_B\left(1-\frac{\gamma_B P_B^0(T_s)}{P_t}\right)-\gamma_B x_B+\frac{p_{B\infty}}{P_B^0(T_s)}=0 \qquad (5)$$

and

$$a^2=a_0^2-2D_{AM}\left(\frac{\gamma_A x_A}{\rho w_A}\right)\frac{M_A P_A^0(T_s)}{RT_s}(t-t_0) \qquad (6)$$

In addition, if component B is significantly more volatile than A (that is, $\beta < 10^{-3}$), Eq. 5 reduces to

$$\gamma_B x_B=\frac{p_{B_\infty}}{P_B^0(T_\infty)}=a_B \qquad (7)$$

Thus, during the quasi-steady evaporation, the composition of the droplet remains in a dynamic equilibrium with respect to component B in the gas phase, and the difference between the droplet and bulk gas activity of A ($\gamma_A x_A$) drives the evaporation process.

The experiments of the present study involve evaporation of a pure glycerol (A) droplet surrounded by an atmosphere containing ethanol (B) vapor and air (C). Under the experimental conditions ($T_\infty = 25$°C, $P_t = 1$ atm), $P_A^0(T_\infty)/P_t \simeq 2\times 10^{-7}$, and $\beta \simeq 2.1\times 10^{-6}$; thus, it can be safely assumed that the composition of ethanol x_B in a glycerol-ethanol droplet during the quasi-steady evaporation is equal to the equilibrium composition corresponding to the gas-phase activity or saturation ratio a_B. Since, under the experimental conditions, $y_A \leq P_A^0(T_\infty)/P_t \simeq 2\times 10^{-7}$ and $y_B \equiv P_{B_\infty}/P_t$ are nearly independent of the position, the gas-phase effective diffusivity of A can be expressed by:

$$D_{AM}=\left[\left(\frac{1}{D_{AB}}-\frac{1}{D_{AC}}\right)\frac{p_{B_\infty}}{P_t}+\frac{1}{D_{AC}}\right]^{-1} \qquad (8)$$

The above relation justifies the assumption of constant gas mixture diffusivities.

Equation 6 shows that during the evaporation of a droplet containing a relatively nonvolatile component in the presence of a volatile vapor, the square of the radius changes linearly with time with a slope of:

$$S=-2D_{AM}\left(\frac{\gamma_A x_A}{\rho w_A}\right)\frac{M_A P_A^0(T_\infty)}{RT_\infty}. \qquad (9)$$

In a vapor-free atmosphere, which corresponds to evaporation of a pure droplet of A ($x_A = 1$, $\gamma_A = 1$, $\rho = \rho_A$, $w_A = 1$, and $D_{AM} = D_{AC}$), the relation for the slope simplifies to

$$S_0=-2D_{AC}\frac{M_A P_A^0(T_\infty)}{\rho_A RT_\infty} \qquad (10)$$

Equations 7 and 9 show that if the composition and evaporation rate (slope of a^2 vs. t data) of a droplet are measured simultaneously, then independent estimates of activity coefficients of both components can be obtained from the measured data. These equations are the bases for the interpretation of experimental data of the present study. It should be pointed out that errors in the activity coefficient estimates due to uncertainties in physical properties or any random fluctuations of experimental conditions can be minimized by collecting data on the same droplet at varying gas phase activity of B. The data can then be analyzed on the basis of the evaporation rate slope ratio which is given by:

$$S_R=\frac{S}{S_0}=\frac{D_{AM}\gamma_A x_A \rho_A}{D_{AC} w_A \rho}. \qquad (11)$$

The above equation shows that the activity coefficient estimates are affected neither by the experimental temperature nor by the total pressure fluctuations, and nor by the uncertainty in the vapor pressure of A.

Experimental Studies

The experimental system used in this study is shown in Figure 1. The salient features of the system have been described in detail by Ray et al. (1989, 1991); here we will present a brief discussion on the system. An electrodynamic balance mounted inside a temperature controlled chamber is used to suspend single droplets in a gas stream. The balance consists of two central ring electrodes and two endcap ring electrodes above and below the central ring electrodes. A variable AC potential on the central ring electrodes focuses a droplet to the center of the balance, while a bipolar DC potential applied across the top and bottom electrodes balances the vertical forces acting on the droplet. This design facilitates unhindered flow of a gas stream through the balance. The following force balance relation applies to a droplet at the center of the balance:

$$4\pi a^3 \rho g/3 = 2KqV_{dc}+6\pi a\mu v. \qquad (12)$$

A suspended droplet is illuminated by a vertically polarized He-Ne laser beam, and the intensity of light scattered by the droplet is detected by a photo-multiplier tube (PMT) mounted on the horizontal plane containing the droplet. The ethanol activity in the gas stream flowing past the suspended droplet is controlled by mixing an ethanol saturated air stream with a dry air stream at an appropriate ratio. The ethanol saturated air is generated by passing dry air through an evaporator-condenser system. The air stream leaving the evaporator is passed through a two-stage falling film condenser. The second stage operates isothermally, and the air stream leaving this stage is saturated with ethanol at the condenser outlet temperature. The flow rates are maintained by micropro-

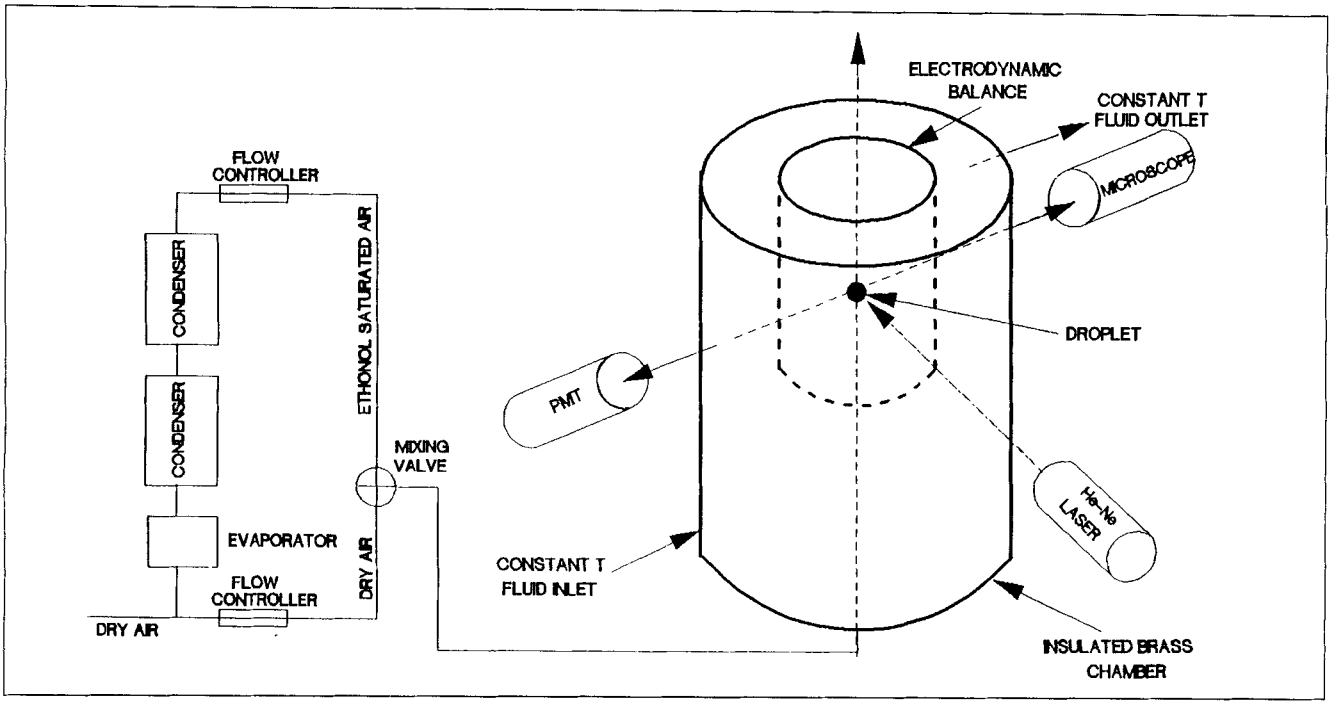

Figure 1. Experimental system.

cessor controlled flowmeters, and prior to introduction to the chamber, the temperature of the mixed gas stream is brought to the chamber temperature by passing it through a heat exchanger.

In a typical experiment, a pure glycerol droplet was suspended in a dry air stream at 25°C. A spectrophotometric grade glycerol (purity > 99.5%) obtained from Aldrich Chemicals was used. Before the start of the experiment the droplet was dried for a few minutes to remove volatile impurities such as water. Then the intensity of scattered light and DC voltage required to balance the droplet were recorded as functions of time. After collecting sufficient data in dry air, the activity of ethanol in the air stream was increased in steps. After each step increase in the ethanol activity, the droplet grew to a maximum size by absorbing ethanol vapor and then evaporated. Only the data collected during the quasi-steady evaporation were used in the analysis.

Data Reduction

In this study, the intensity of scattered light vs. time data are analyzed using Lorenz-Mie theory to obtain the size and refractive index (composition) of an evaporating droplet responsible for the scattered intensity spectrum. Here, we shall present a brief review of the theoretical basis for the interpretation of light scattering data, and then describe the procedure used for determining compositions and evaporation rates.

Light scattering by spherical particle

When a spherical particle is illuminated by a vertically polarized monochromatic beam of wavelength λ, the far-field intensity of scattered light in the horizontal scattering plane is given by (van de Hulst, 1981; Kerker, 1983; Bohren and Huffman, 1983):

$$I = \frac{I_i \lambda^2}{4\pi^2 r^2}\left\{\sum_{n=1}^{\infty}\frac{2n+1}{n(n+1)}\left[a_n\frac{P_n^1(\cos\theta)}{\sin\theta} + b_n\frac{d}{d\theta}P_n^1(\cos\theta)\right]\right\}^2 \quad (13)$$

where θ, the angle between the incident light direction and the scattering direction, is called the scattering angle. In the present study θ corresponding to the PMT position is calibrated to an accuracy of 0.05°. For a homogeneous sphere of radius a, the scattering coefficients a_n and b_n of the transverse electric (TE) and magnetic (TM) modes depend on the size parameter, defined by $X = 2\pi a/\lambda$, and the refractive index of the sphere relative to the surrounding medium m. The coefficients may be written in the following forms:

$$a_n = \frac{A_n(X,m)}{A_n(X,m) + \iota C_n(X,m)} \quad (14)$$

and

$$b_n = \frac{B_n(X,m)}{B_n(X,m) + \iota D_n(X,m)}, \quad (15)$$

where A_n, B_n, C_n and D_n are related to Riccati-Bessel functions of first and second kinds with arguments X and mX (Bohren and Huffman, 1983).

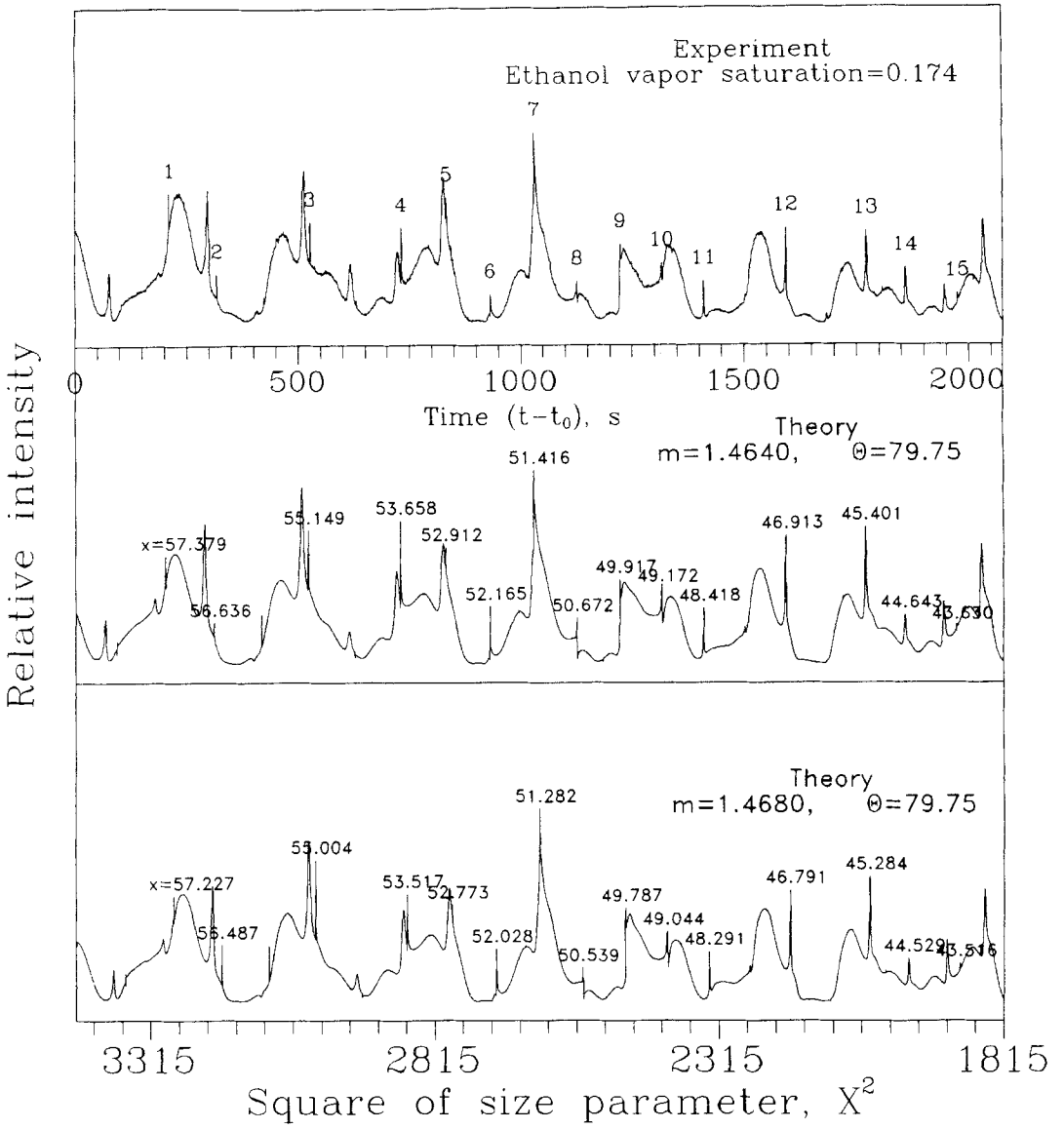

Figure 2. Experimental intensity vs. time data with theoretical intensity spectra for two refractive indices.

At a fixed scattering angle, the scattered intensity as a function of size parameter shows sharp peaks, called resonances, superimposed on a slowly varying intensity profile. Resonances occur for values of X and m for which the imaginary part of the denominator of one of the scattering coefficients goes to zero, and the coefficient itself attains a maximum value of 1. The locations of resonances can be computed from the roots of $C_n(X,m)=0$ for a TM coefficient (that is, a_n) and $D_n(X,m)=0$ for a TE coefficient. These resonances are identified by the mode number n and an order number ℓ, where the first root is labeled $\ell=1$.

Experimentally, an intensity spectrum is obtained either by varying the incident wavelength (Ray and Huckaby, 1993) or by varying the size of a droplet illuminated by a fixed wavelength light (Richardson et al., 1986; Taflin et al., 1988; Ray et al., 1989, 1991). For given m and θ, the shape of an intensity spectrum is unique and depends on the size parameter interval. By matching the shape of an experimental spectrum with a theoretical spectrum, and by identifying the resonances responsible for the observed intensity peaks, the size of a spherical particle can be obtained with high precision.

Composition and evaporation rate determination

A typical intensity vs. time spectrum obtained from a glycerol droplet evaporating in 17.4% ethanol saturated air is shown in Figure 2. In previous studies, such spectra obtained from evaporating droplets have been visually matched with theoretical spectra to obtain size and/or refractive index vs. time information (Richardson et al., 1986; Taflin et al., 1988; Ray et al., 1989, 1991; Allen et al., 1990). The visual matching is only accurate for situations in which the refractive index of the droplet and the functional form of the size variation with time are known. For example, the size or the square of the size varies linearly with time in the kinetic or continuum regime evaporation of a single component droplet. In those

situations, intensity vs. time spectra can be visually matched with theoretical spectra of intensity vs. size parameter (Richardson et al., 1986) or square of the size parameter (Ray et al., 1989) to obtain size vs. time data.

For the present experiments, Eq. 6 provides the functional form of the size variation. The problem involves determination of the refractive index and slope of a^2 vs. t data from an intensity spectrum obtained from a droplet evaporating in a partially saturated ethanol vapor. The shape of a theoretical spectrum is not sensitive to the refractive index. An example is provided in Figure 2 which compares the experimental spectrum with theoretical intensity vs. X^2 spectra for $m = 1.464$ and 1.468. The experimental intensity spectrum agrees visually equally well with both theoretical spectra, and indeed, such an agreement holds true for any theoretical spectrum in the range $1.464 \le m \le 1.468$. Any one of the theoretical spectra in that refractive range can conceivably be the true match for the observed spectrum. A visual match, thus, provides a refractive index range for the observed spectrum. Conversely, the refractive index can be determined with a degree of uncertainty (such as $m = 1.466 \pm 0.002$ for the spectrum in Figure 2.)

To further narrow the refractive index range we have adopted an optimization procedure based on the alignment of experimental peaks with theoretical peaks. The experimental data provide the time of occurrence $t_{k,\text{obs}}$, of each of the observed peaks labeled, say, $k = 1$ to N. We also know that the size of an evaporating droplet is governed by Eq. 6 which in terms of the size parameter can be written as:

$$X^2 = X_0^2 - b(t - t_0) \tag{16}$$

The problem now involves determination of three parameters: X_0, b and m. The procedure for the determination of optimum values of these parameters can be understood by considering Figure 2 where the sharp peaks in the experimental spectrum are labeled 1 to 15, and the size parameter values of the corresponding peaks in the theoretical spectra are also shown. Figure 2 shows that the size parameter values of all the theoretical peaks increase as the refractive index decreases from 1.468 to 1.464, and the magnitude of increase varies from peak and peak. Thus, for each observed peak a visual match provides a unique relation between its position (size parameter value) and refractive index. The uniqueness arises from the fact that a visual match identifies the mode and order numbers of the observed peaks whose positions can be calculated from $C_n(x, m) = 0$ or $D_n(x, m) = 0$. Thus, we have a relation for the position of an observed peak as a function of m, that is

$$X_k = f(m, n_k, \ell_k), \tag{17}$$

where n_k and ℓ_k are the order and mode numbers of kth peak determined from the visual match. Equation 17 shows that for an assumed refractive index we can calculate the position of a resonance peak observed at time $t_{k,\text{obs}}$. This procedure is used to generate X_k vs. $t_{k,\text{obs}}$ data which are then regressed to Eq. 16, using a least-squares method, to obtain the best estimates of parameters X_0 and b for the assumed refractive index value. The resulting formula (Eq. 16) is then

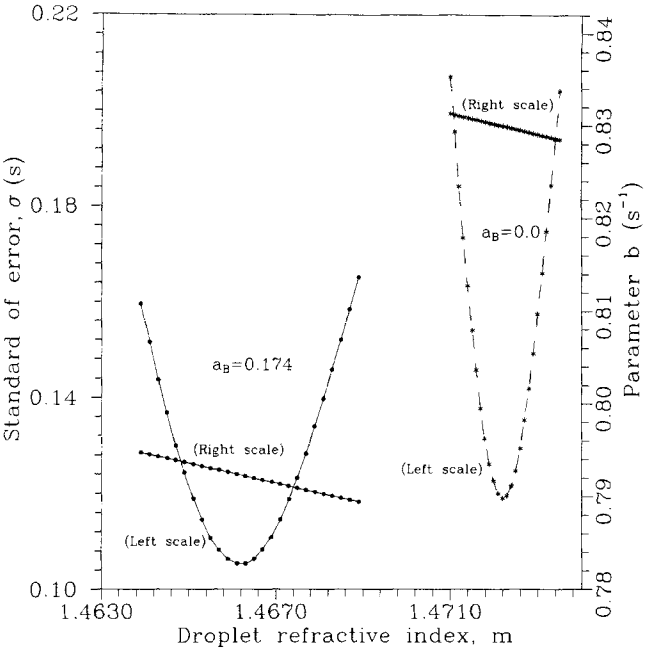

Figure 3. Peak alignment error and evaporation rate parameter b vs. refractive index data for two evaporating droplets.

used to calculate $t_{k,\text{cal}}$, the time of occurrence of kth peak, and the alignment error between the observed and calculated peak occurrence times is estimated using the following relation:

$$\text{ES}(m) = \sum_{k=1}^{N} (t_{k,\text{obs}} - t_{k,\text{cal}})^2 \tag{18}$$

Using a computer program, these steps are repeated by changing the refractive index value, and the minimum in the error estimate is obtained. The values of X_0, b and m at the minimum are the best estimates.

The results obtained, using the times corresponding to the peaks labeled 1 to 15 in Figure 2, are shown in Figure 3. Here we have plotted values of standard error σ and parameter b as functions of the refractive index. The results show that the error is a continuous function of m and has one distinct minimum which occurs at $m = 1.4661$. Moreover, the parameter b decreases as m increases, and at the minimum error it has a value of $b = 0.7924\ \text{s}^{-1}$, which corresponds to an evaporation rate (slope of a^2 vs. t) of $8.037 \times 10^{-3}\ \mu\text{m}^2/\text{s}$ in air with ethanol vapor at a saturation ratio of 0.174.

The validity and sensitivity of the optimization procedure are demonstrated by the results obtained from a glycerol droplet evaporating in ethanol-free air. Figure 3 shows that the error minimum for that droplet occurs at $m = 1.4722$ and the corresponding value of b is $0.8299\ \text{s}^{-1}$. The optimum refractive index value agrees well with the measured value of 1.4720 for bulk glycerol samples. Moreover, the evaporation rate of $8.418 \times 10^{-3}\ \mu\text{m}^2/\text{s}$ at the optimum refractive index compares well with $(8.51 \pm 0.10) \times 10^{-3}\ \mu\text{m}^2/\text{s}$, the data reported by Ray et al. (1989). These facts and the shapes of the

error vs. m plots lead us to conclude that the refractive index can be determined with an accuracy of 3 parts in 10^4. Since the refractive indices of pure glycerol and ethanol are 1.4722 and 1.3611, respectively, we can resolve the composition of a droplet by about 3 parts in 10^3. As mentioned before, the refractive index and slope estimations are interrelated; thus, an error of $\pm 3\times 10^{-4}$ in the refractive index introduces an error of 0.04% in the simultaneous slope determination.

To determine the composition from the refractive index value, we have used the following molar refractivity relation for a binary solution (Born and Wolf, 1989):

$$\frac{M}{\rho}\frac{m^2-1}{m^2+2} = R_A x_A + R_B x_B \tag{19}$$

To estimate molar refractivities we have measured refractive indices of glycerol-ethanol mixtures at various compositions, and regressed the data to Eq. 19 to obtain $R_A = 0.020575$ and $R_B = 0.012909$. The solution density has been calculated from the following polynomial obtained by fitting the density vs. weight fraction data reported by Washburn (1928):

$$\rho = 1253.43 - 667.22 w_B + 387.53 w_B^2 - 183.58 w_B^3 \tag{20}$$

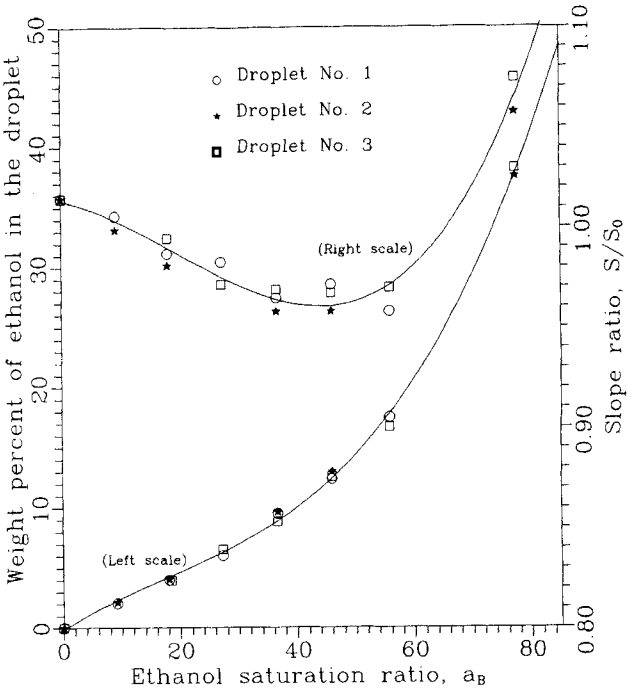

Figure 4. Measured droplet compositions and evaporation rate slope ratios at various ethanol saturation ratios.

Results and Discussions

In a typical experiment, the data were first obtained on a pure glycerol droplet evaporating in an ethanol-free air stream. Then the same droplet was exposed in steps to air streams containing ethanol vapor at various saturation ratios. The experimental ethanol weight fraction and slope ratio vs. ethanol saturation ratio data, obtained from three droplets, are shown in Figure 4. At a given saturation ratio, the maximum difference between the weight fractions observed in any two droplets is less than 1%, while the measured slope ratios differ at most by 2%. Thus, the experimental data are reproducible.

The experimental data of the present study represent independent measurements of three quantities: ethanol saturation ratio a_B, composition x_B and slope ratio S_R at constant T. For the flow rate and droplet size range involved in the study, the maximum value of the Sherwood number has been estimated to be 2.008. Thus, for the analysis of the data, Eqs. 7 and 11, obtained by considering a stagnant medium, can be applied without any correction. For calculations, we have used diffusion coefficient values $D_{AC} = 9.14\times 10^{-6}$ m^2/s and $D_{AB} = 5.97\times 10^{-6}$ m^2/s, estimated from the relation of Fuller et al. (1966). It should be noted that small errors in the diffusion coefficient estimates introduce only negligible errors in the glycerol activity calculated from Eq. 11 since the diffusivity ratio computed from Eq. 8 varies only from 0.97 to 1 for ethanol saturation ratios involved in the experiments.

Since the experimental $\gamma_B x_B - x_B - \gamma_A x_A$ data imply over-determination of thermodynamic vapor-liquid equilibrium parameters for glycerol-ethanol system, we can obtain parameters of a Gibbs free energy model as well as test our data for thermodynamic consistency. To this purpose, we have followed the procedure recommended by Van Ness et al. (1973), using the following forms of the Margules and Wilson equations:

$$\frac{g^E}{RT} = x_A \ln\gamma_A + x_B \ln\gamma_B$$

$$= (Ax_B + Bx_A)x_A x_B \qquad \text{Margules} \tag{21}$$

$$= -x_A \ln(x_A + Ax_B) - x_B \ln(x_B + Bx_A) \qquad \text{Wilson} \tag{22}$$

We have fitted the experimental data to these equations using all the experimental data; $\gamma_B x_B - x_B$ data; $\gamma_A x_A - x_B$ data; and $\gamma_B x_B - \gamma_A x_A$ data, and minimized the following objective functions to obtain the best estimates of parameters A and B:

$$\text{O.F.} = \sum_i \left(y^j_{i,\text{exp}} - y^j_{i,\text{cal}}(x_B, A, B)\right)^2 \tag{23}$$

where

$$y_i^1 = \left(\frac{g^E}{RTx_A x_B}\right)_i,$$

$$y_i^2 = (\gamma_A x_A)_i,$$

$$y_i^3 = (\gamma_B x_B)_i,$$

and

$$y_i^4 = (\gamma_A x_A)_i.$$

Table 1. Margules Equation Constants Obtained from Four Data Subsets

Model	Data Used	Parameters A	Parameters B	RMS Deviation $\Delta\gamma_A x_A$	RMS Deviation $\Delta\gamma_B x_B$
Margules	$\gamma_A x_A - \gamma_B x_B - x_B$	1.525	0.856	0.011	0.009
	$\gamma_B x_B - x_B$	1.574	0.844	0.013	0.009
	$\gamma_A x_A - x_B$	1.467	0.689	0.005	0.019
	$\gamma_A x_A - \gamma_B x_B$	1.459	0.824	0.011	0.012
Wilson	$\gamma_A x_A - \gamma_B x_B - x_B$	0.131	0.970	0.010	0.012
	$\gamma_B x_B - x_B$	0.181	0.898	0.012	0.009
	$\gamma_A x_A - x_B$	0.139	0.986	0.009	0.014
	$\gamma_A x_A - \gamma_B x_B$	0.140	0.966	0.010	0.011

For the first three data sets, the calculated quantities in the objective functions have been estimated using the experimentally determined values of composition. Since the last data subset involves $\gamma_A x_A$ vs. $\gamma_B x_B$ data, we have first calculated compositions by equating measured activities of B with calculated values, that is, from the relation:

$$(\gamma_B x_B)_{\text{cal}} = (\gamma_B x_B)_{\text{exp}}, \tag{24}$$

and then used the calculated values of composition in the objective function.

The best estimates of parameters A and B obtained from the analyses of four subsets of data are listed in Table 1. The results show that the parameter values depend on the choice of data subset, and vary significantly from one set to another. However, the quality of the data can only be judged by comparing the measured quantities with values predicted by these sets of parameters, and from deviations among predicted values. The root-mean-square (RMS) deviations between the measured and calculated activities are shown in Table 1. Calculations based on both the Margules and Wilson equations predict similar levels of deviations. Figure 5 compares the experimental $\gamma_A x_A$ and $\gamma_B x_B$ vs. x_B data with the predictions from the Margules equations with four sets of parameter values listed in Table 1. The results show that the predictions from any one of the four sets differ from the predictions from the other sets at most by 4%. The parameters from $\gamma_B x_B - x_B$ data predict highest values of $\gamma_A x_A$ and $\gamma_B x_B$, while the parameters from $\gamma_A x_A - x_B$ data predict the lowest values. The predictions from the other two data subsets lie in between these extreme values. Due to the nature of the objective functions, the measured activities of A and B agree with the lower and upper extremes of the predicted values, respectively.

The real proof of thermodynamic consistency lies in the ability of the parameters obtained from any two of the measured quantities to predict the third measured quantity (Prausnitz et al., 1986). When the parameters obtained from $\gamma_B x_B - x_B$ data are used, RMS deviations between the measured and calculated values of $\gamma_A x_A$ based on the Margules and Wilson equations are 0.013 and 0.012, respectively. When $\gamma_A x_A - x_B$ data are used RMS deviations in $\gamma_B x_B$ are slightly higher. Similarly, for the $\gamma_A x_A - \gamma_B x_B$ data the measured activities of A and B deviate on the average from the calculated activities at the measured compositions by about 0.011. In these three cases, the maximum deviation between the calculated and measured quantities is less than 0.035. Thus, on the basis of the RMS and maximum deviations, we can conclude that the data are thermodynamically consistent. However, the deviations are somewhat larger than expected on the basis of the accuracies involved in the composition and slope determination, and can be attributed mostly to inaccuracies in ethanol activity measurements, as discussed in the conclusions section.

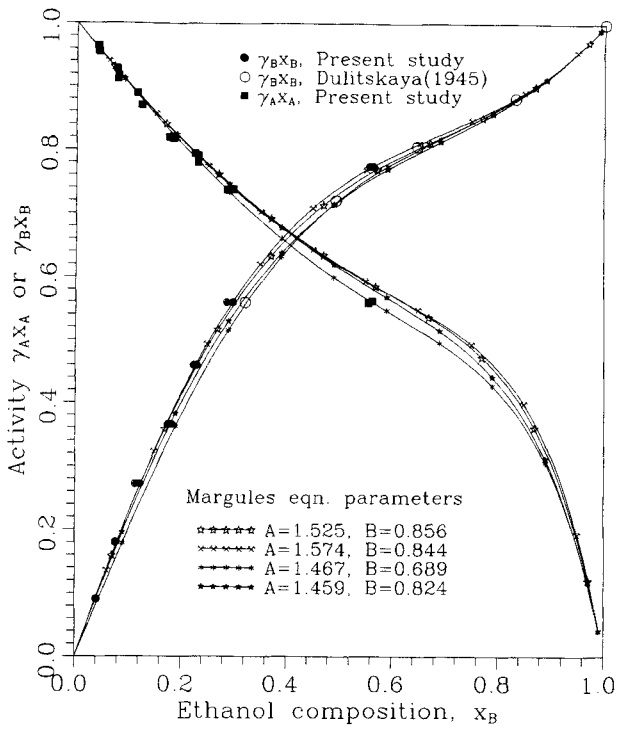

Figure 5. Experimental vs. predicted activity values.

To examine the ability of the present data to predict the results of another study in Figure 5, we have compared the measured ethanol activity vs. composition data of Dulitskaya (1945) with the predictions from the present study. The ethanol activity values of Dulitskaya have been calculated from the total pressure vs. ethanol mole fraction data reported by Gmehling et al. (1977). The comparison shows that the maximum deviation between Dulitskaya's data and calculated values based on four data subsets is less than 4%. The parameter based $\gamma_A x_A - x_B$ data most accurately predict Dulitskaya's $\gamma_B x_B$-x_B data (the average and maximum deviations are less than 0.01), while the measured and predicted values of $\gamma_B x_B - \gamma_B$ data of the present study deviate most from Dulitskaya's data, again suggesting higher levels of error in ethanol saturation ratio measurements.

Conclusions

A technique, based on the evaporation of a binary droplet in a controlled vapor phase, has been demonstrated to be capable of determining activity coefficients of components that markedly differ in volatility. The experimental $\gamma_A x_A$-$\gamma_B x_B$-x_B data on the glycerol-ethanol system have been analyzed by considering all three measured variables as well as

using three different combinations of two measured variables at a time. The analyses show that both the Margules and Wilson equations examined here can describe the experimental data, and that the data are thermodynamically consistent. The values of glycerol activity computed from the measured ethanol activity vs. composition data agree with the measured values. A similar agreement is also observed when the measured glycerol activity vs. composition data are used to predict the measured values of ethanol activity. The maximum deviation between the calculated and measured values is less than 0.035. The results of the present study also agree with the data reported in the literature. In particular, the values of ethanol activity calculated from the measured glycerol activity vs. composition data are almost identical to the reported values.

The light scattering technique used here can determine refractive index of a droplet with an accuracy of ± 0.0003, and the slope of a^2 vs. t data with 0.04%. Thus, the absolute errors in the composition and glycerol activity determination are likely to be less than 0.05. These accuracies are reflected in the agreement between the ethanol activity values reported in the literature and the values calculated from the measured glycerol activity vs. composition data. Although the thermodynamic consistency of the data and the agreement between the present data and literature data are reasonably good, the ethanol activity data deviate most from the calculated as well as from the reported values. This leads us to believe that most of the experimental errors are associated with ethanol activity measurements. The results suggest that the measured ethanol saturation ratios are consistently higher, on the average by about 2% and at most by 3.5%, than the values reported in the literature as well as predicted from the analysis based on $\gamma_A x_A - x_B$ data. The ethanol saturation ratios have been determined from the temperature of the saturated stream leaving the condenser and the volumetric flow rate ratio of ethanol-saturated to ethanol-free air streams. The condenser outlet temperature measurement is accurate to $\pm$ 0.1 K, and an error of 0.1 K introduces an error of about 0.6% in the ethanol saturation ratio. Finally, the adsorption and absorption of ethanol vapor in the tubing between the condenser and chamber may have reduced the ethanol vapor saturation ratio actually encountered by a droplet. These problems can be considerably mitigated and the accuracy of determination of activity of the volatile component can be significantly improved by directly measuring the vapor concentration close to the inlet and/or outlet of the chamber, using, for example, a chilled mirror dew point sensor.

A major advantage of the present technique is that the activity coefficients of both components can be determined over a wide range of composition from an experiment on a single droplet. The technique is not limited only to binary systems containing components that differ markedly in volatility. The theoretical basis of the technique lies in the fact that a binary droplet in the presence of the more volatile vapor evaporates as a constant composition droplet. The activity coefficients of both components and the droplet temperature can be determined if the evaporation rate, droplet composition and activity of the vapor-phase component are measured independently. Thus, the technique has no upper or lower limits on the relative volatility of the system, but it is particularly useful for systems containing a fairly nonvolatile component whose activity coefficient cannot be determined using conventional techniques.

The sensitivity of composition determination in the present technique depends on the liquid-phase refractive index difference between the individual components of the binary system. When the refractive indices are close to each other, the composition cannot be determined from the refractive index. However, for such systems the evaporation rate can still be obtained accurately from light-scattering data, and the droplet density (composition) from the balancing DC voltage data using Eq. 12. If the system contains a fairly nonvolatile component such that the evaporation rate is sufficiently slow, a more precise light scattering technique based on varying incident wavelength may be adopted. Ray and Huckaby (1993) have shown that such a technique can detect size changes as low as 1 nm and the absolute refractive index with a resolution of one part in 10^5.

Acknowledgment

The authors are grateful to the National Science Foundation (grant No. CTS-9309055), Dept. of Energy, U. S. Army Chemical RD&E Center and Brown and Williamson Tobacco Corp. for their generous support.

Notation

a = droplet radius, μm
a_i = gas-phase activity or saturation ratio
a_n = scattering coefficient in Eq. 14
A = parameter in Eq. 21
$b = 2D_{AM}\left(\frac{2\pi}{\lambda}\right)^2\left(\frac{\gamma_A x_A}{\rho w_A}\right)\frac{M_A P_A^0(T_\infty)}{RT}$, parameter in Eq. 16, s^{-1}
b_n = scattering coefficient in Eq. 14
B = parameter Eq. 21
c_t = gas-phase total molar density, kmol/m^3
$C_{pM} = (x_A C_{pA} + x_B C_{pB})$, gas-phase molar heat capacity, J/kmol·K
D_{ij} = gas-phase diffusivity, m^2/s
ES = sum of error squares, s^2
g = acceleration due to gravity, m/s^2
g^E = excess Gibbs free energy
I = intensity of light, W/m^2
k_j = gas-phase thermally conductivity, W/m·K
K = electrodynamic balance constant
$Le = D_{AM} c_t C_{pM}/k_M$, Lewis number
m = droplet refractive index
M = average molecular weight of solution
M_i = molecular weight of component i
N = number of resonance peaks
N_A = molar flux of component A, mol/m^2·s
p_i, P_i°, P_t = partial vapor and total pressure respectively, Pa
q = Columbic charge on a droplet, C
R = gas constant, J/kmol·K
R_i = molar refractivity, m^3/kmol
S = slope of a^2 vs. t data, μm^2/s
S_R = slope ratio defined by Eq. 11
t = time, s
T = temperature, K
v = gas velocity around a droplet, m/s
V_{dc} = DC potential on endcap electrodes
w_i = weight fraction
x_i = liquid-phase mole fraction
X = potential size parameter

Greek letters

$\beta = D_{AM}P_A^\circ/D_{BM}P_B^\circ$, parameter in Eq. 5
γ_i = activity coefficient
$\Delta H_{vM} = (x_A \Delta H_{vA} + x_B \Delta H_{vB})$, heat of vaporization, J/kmol
θ = scattering angle corresponding to PMT position, rad
λ = wavelength of incident light, μm
μ = gas-phase viscosity, kg/m·s
ρ = solution density, kg/m^3
ρ_i = liquid-phase density of i, kg/m^3

Subscripts

A, B, C = components
i, j = components
k = kth labeled peak
ℓ = resonance order number
M = gas mixture
n = resonance mode number
o = initial value
s = droplet surface
∞ = bulk gas

Literature Cited

Allen, T. M., D. C. Taflin, and E. J. Davis, "Determination of Activity Coefficients via Microdroplet Evaporation Experiments," *Ind. Eng. Chem. Res.*, **29**, 682 (1990).

Bohren, C. F., and D. R. Huffman, *Absorption and Scattering of Light by Small Particles*, Interscience, New York (1983).

Born, M., and E. Wolf, *Principles of Optics*, Pergamon, Oxford (1989).

Cheong, W. J., and P. W. Carr, "Limiting Activity Coefficients and Gas-Liquid Partition Coefficients of Alkylbenzenes in Hydroorganic Solvents," *J. Chromat.*, **500**, 215 (1990).

Cohen, M. D., R. C. Flagan, and J. H. Seinfeld, "Studies of Concentrated Electrolyte Solutions Using the Electrodynamic Balance: 1. Water Activities for Single Electrolyte Solutions," *J. Phys. Chem.*, **91**, 4563 (1987a).

Cohen, M. D., R. C. Flagan and J. H. Seinfeld, "Studies of Concentrated Electrolyte Solutions Using the Electrodynamic Balance: 2. Water Activities for Mixed Electrolyte Solutions," *J. Phys. Chem.*, **91**, 4575 (1987b).

Donohue, M. D., D. M. Shah, and K. G. Connally, "Henry's Constants for C_5 to C_9 Hydrocarbons in C_{10} and Larger Hydrocarbons," *Ind. Eng. Chem. Fund.*, **24**, 241 (1985).

Dulitskaya, K. A., *Zh. Obshch. Khim*, **15**, 9 (1945).

Eckert, C. A., B. A. Newman, G. L. Nicolaides, and T. C. Long, "Measurement and Application of Limiting Activity Coefficients," *AIChE J.*, **27**, 33 (1981)

Fuller, E. N., P. D. Schettler, and J. C. Giddings, "A New Method for Prediction of Binary Gas-Phase Diffusion Coefficients," *Ind. Eng. Chem.*, **58**, 18 (1966)

Gmehling, J., U. Onken, and J. R. Rarey-Nies, *Vapor-Liquid Equilibrium Data Collection*, DECHEMA Chemistry Data Ser., Vol. I/2e, DECHEMA, Frankfurt (1977).

Hackenberg, H., and A. P. Schmidt, *Gas Chromatographic Headspace Analysis*, Heyden & Son, London (1976).

Huckaby, J. L., and A. K. Ray, "Absorption of Sulfur Dioxide by Growing and Evaporating Water Droplets," *Chem. Eng. Sci.*, **44**, 2797 (1989).

Kerker, M., *The Scattering of Light and Other Electromagnetic Radiation*, Academic Press, New York (1983).

Kurtz, C. A., and C. B. Richardson, "Measurement of Phase Changes in a Microscopic Lithium Iodide Particle Levitated in Water Vapor," *Chem. Phys. Lett.*, **109**, 190 (1984).

Li, J.-D., Y.-G. Li, J. Chen, J.-F. Lu, and T. Teng, "Activity Coefficient Data and Their Correlation for Tributyl-Phosphate-Hydrocarbon and Uranyl Nitrate Tributyl Phosphate Complex-Hydrocarbon Solutions," *Fluid Phase Equilib.*, **58**, 307 (1990).

Lobien, G. M., and J. M. Prausnitz, "Infinite-Dilution Activity Coefficient from Differential Ebulliometry," *Ind. Eng. Chem. Fund.*, **21**, 109 (1982).

Malik, K. L., *An Introduction to Nonanalytical Applications of Gas Chromatography*, Peacock Press, New Delhi (1976).

Newbold, F. R., and N. R. Amundson, "A Model for the Evaporation of a Multicomponent Droplet," *AIChE J.*, **19**, 22 (1973).

Palczewka-Tulinska, M., D. Wyrzykowska-Stankiewicz, J. Cholinski, and K. Zieborak, "Isobaric Vapor-Liquid Equilibrium in Two Binary Systems Involving tert-Amyl Methyl Ether," *Fluid Phase Equilibr.*, **54**, 57 (1990).

Pescar, R. E., and J. J. Martin, "Solution Thermodynamics from Gas-Liquid Chromatography," *Anal. Chem.*, **38**, 1661 (1966).

Prausnitz, J. M., R. N. Lichtenthaler, and E. Gomes de Azevedo, *Molecular Thermodynamics of Fluid-Phase Equilibria*, 2nd ed., Prentice Hall, Englewood Cliffs, NJ (1986)

Ray, A. K., R. D. Johnson, and A. Souyri, "Dynamic Behavior of Single Glycerol Droplets in Humid Air Streams," *Langmuir*, **5**, 133 (1989).

Ray, A. K., B. Devakottai, A. Souyri, and J. L. Huckaby, "Evaporation Characteristics of Droplets Coated with Immiscible Layers of NonVolatile Liquids," *Langmuir*, **7**, 525 (1991).

Ray, A. K., A. Souyri, E. J. Davis, and T. M. Allen, "Precision of Light Scattering Techniques for Measuring Optical Parameters of Microspheres," *Appl. Optics*, **30**, 3974 (1991).

Ray, A. K., and J. L. Huckaby, "Absorption of Sparingly Solute Vapor in Microdroplets: A Study Based on Light Scattering," *Langmuir*, **9**, 2225 (1993).

Renninger, G. R., F. G. Hiller, and R. C. Bone, "The Evaporation and Growth of Droplets Having More Than One Volatile Constituent," *J. Aerosol Sci.*, **12**, 505 (1981).

Richardson, C. B., and C. A. Kurtz, " A Novel Isopiestic Measurement of Water Activity in Concentrated and Supersaturated Lithium Halide Solutions," *J. Amer. Chem. Soc.*, **106**, 6615 (1984).

Richardson, C. B., and J. F. Spann, "Measurement of Water Cycle in a Levitated Ammonium Sulfate Particles," *J. Aerosol Sci.*, **15**, 563 (1984).

Richardson, C. B., R. L. Hightower, and A. L. Piggs, "Optical Measurements of the Evaporation of Sulfuric Acid Droplets," *Appl. Optics*, **25**, 1226 (1986).

Smolik, J., and J. Vitovec, "Quasistationary Evaporation of a Droplet into a Multicomponent Gases MIxture," *J. Aerosol Sci.*, **15**, 545 (1984).

Swietoslawski, W. *Ebulliometric Measurements*, 3rd ed., Reinhold, New York (1945).

Taflin, D. C., S. H. Zhang, T. Allen, and E. J. Davis, "Measurement of Droplet Interfacial Phenomena by Light-Scattering Technique," *AIChE J.*, **34**, 1310 (1988).

Tang, I. N., H. R. Munkelwitz and N. Wang, "Water Activity Measurements with Single Suspended Droplets: The NaCl-H_2O and KCl-H_2O Systems," *J. Colloid Interface Sci.*, **114**, 409 (1986).

Trampe, D. M., and C. A. Eckert, "Calorimetric Measurement of Partial Molar Excess Enthalpy at Infinite Dilution," *J. Chem. Eng. Data*, **36**, 112 (1991).

Trampe, D. M., and C. A. Eckert, "A Dew Point Technique for Limiting Activity Coefficients in Nonionic Solutions," *AIChE J.*, **39**, 1045 (1993).

van de Hulst, H. C., *Light Scattering by Small Particles*, Dover, New York (1981).

Van Ness, H. C., S. M. Byer, and R. E. Gibbs, "Vapor-Liquid Equilibrium: I. An Appraisal of Data Reduction Method," *AIChE J.*, **19**, 238 (1973).

Vijayaragahaven, B., "Evaporation and Growth Kinetics of Multicomponent and Multilayered Droplets," MS Thesis, Univ. of Kentucky, Lexington, KY (1990).

Washburn, E. W., *International Critical Tables of Numerical Data, Physics Chemistry and Technology*, Vol. III, McGraw-Hill, New York (1928).

Manuscript received Jan. 6, 1994, and revision received May 16, 1994.